# Valence Electron - Noble Gas Atom Pseudopotentials for Atomic Spectral Line Shape Calculations

John Kielkopf

December 1, 2019

**Abstract**

A pseudopotential for computing the long range interaction of a hydrogenic atom with a noble gas atom is described that is based on fundamental physics and meaningful model parameters. The development of this approach is outlined and its relationship with other similar methods is explained, while the benefit of its simplicity enables predictive rapidly executed computation. A central component is the use of atomic basis states which asymptotically represent the unperturbed hydrogenic atom. The mixing of these states, which can span different principle quantum numbers or configurations, shows how collision-induced changes in transition probability affect the far line wing profiles of atomic transitions. Examples are provided for H, Na, K, and Cs with representative perturbing rare gases He, Ar, and Xe. Where possible, comparisons are made with recent data and ab initio calculations that show some of the limitations of both the simpler pseudopotential, and the complex molecular ab intio methods. This code is intended to be part of a comprehensive suite of programs that can predict spectral line shapes due to neutral atomic collisions over a wide range of conditions. An example of H-He is given to show that the blue wing of Lyman-$\alpha$ is collision-induced, while the red wing is collision-suppressed due to state mixing.

# Contents

# Chapter 1

# Atomic spectral line shapes

A single atom isolated from neighbors is described well by a uniquely defined wavefunction with a characteristic energy. Over time, the distribution of photons it may emit or absorb is centers on specific energies that are differences in energy states of the atom, and viewed as wavelength or frequency have come to be called "line" for their appearance visually in a spectrometer. Josef Fraunhofer's study of spectra provided the earliest list of these features in the spectrum of the Sun he saw with prisms and diffraction gratings of his own making. For the purpose of making achromatic telescopes, he measured the index of refraction of various glasses using the lines of the solar spectrum for precise reference wavelengths shown in Fig. 1.1 in an arrangement that became the standard for prism spectrometers for years to come. Figure 1.2 reproduces his hand-drawn map with the now-famous letter designations when they were first published.

The dark lines he discovered had been seen before, notably by William Hyde Wollaston in 1802 who also used them as references for index of refraction measurements. Notably, Wollaston thought they separated the colors of the continuum [50](page 378). Fraunhofer, Bunsen, and Kirchhoff recognized the pair of emission lines they saw when sodium was introduced into a flame were at the same wavelength as the dark lines found in the spectrum of the Sun and labeled "D" in Fraunhofer's map. [21] This and further observations with telescopes of the spectra of bright stars became the foundation for building our understanding of the composition, tempera-

ture, density, rotation, and systemic velocity of stars so distant they appear as unresolved pinpoint sources of light. The D-lines in the Sun arise when an unexcited sodium atom in the $3s$ state absorbs a photon and increases its energy to be momentarily in a $3p$ state. The energetic $3p$ state is unstable to decay by electric dipole radiation, the inverse of the absorption event that excites it, and in about 16 nanoseconds the atom emits a photon and returns to its lowest possible energy again. [42] The departing photon on average may leave in any direction, and consequently is lost to the distant observer who sees a dark or "absorption" line in the spectrum.

## 1.1 Fourier transforms and a spectrum

The connection between a time-dependent atomic process and an observable distribution of photon energies in frequency space is through the Fourier Transform. While the formal definitions and normalizations of the Fourier transform are not standardized, we use a forward transform $\mathcal{F}$ of a function of time $t$ and an inverse transform $\mathcal{F}^{-1}$ of a function of frequency $\nu$ with a normalization and sign convention defined by Brigham ([7], pp. 48-49)

$$H(\nu) = \mathcal{F}(h(t)) \tag{1.1}$$
$$h(t) = \mathcal{F}^{-1}(H(\nu)) \tag{1.2}$$

$$H(\nu) = \int_{-\infty}^{+\infty} h(t) \exp(-i\, 2\pi\nu t) dt \tag{1.3}$$
$$h(t) = \int_{-\infty}^{+\infty} H(\nu) \exp(+i\, 2\pi\nu t) d\nu \tag{1.4}$$

Parseval's theorem then gives

$$\int_{-\infty}^{+\infty} |h^2(t)|\, dt = \int_{-\infty}^{+\infty} |H^2(\nu)|\, d\nu \tag{1.5}$$

Note that with these definitions for the Fourier transform pair, the frequency integration is over $\nu$ rather than over $\omega = 2\,\pi\nu$ common in contemporary physics literature. A transformation $t \to \nu$ of Eq. 1.3 is usually referred to as a *forward* Fourier transform, and one that takes $\nu \to t$ of Eq. 1.4 is an *inverse* Fourier transform. The forward and inverse transforms are mathematically symmetric with our choice of normalization. With the definition used here, the frequency dependent $H(\nu)$ may be used as the

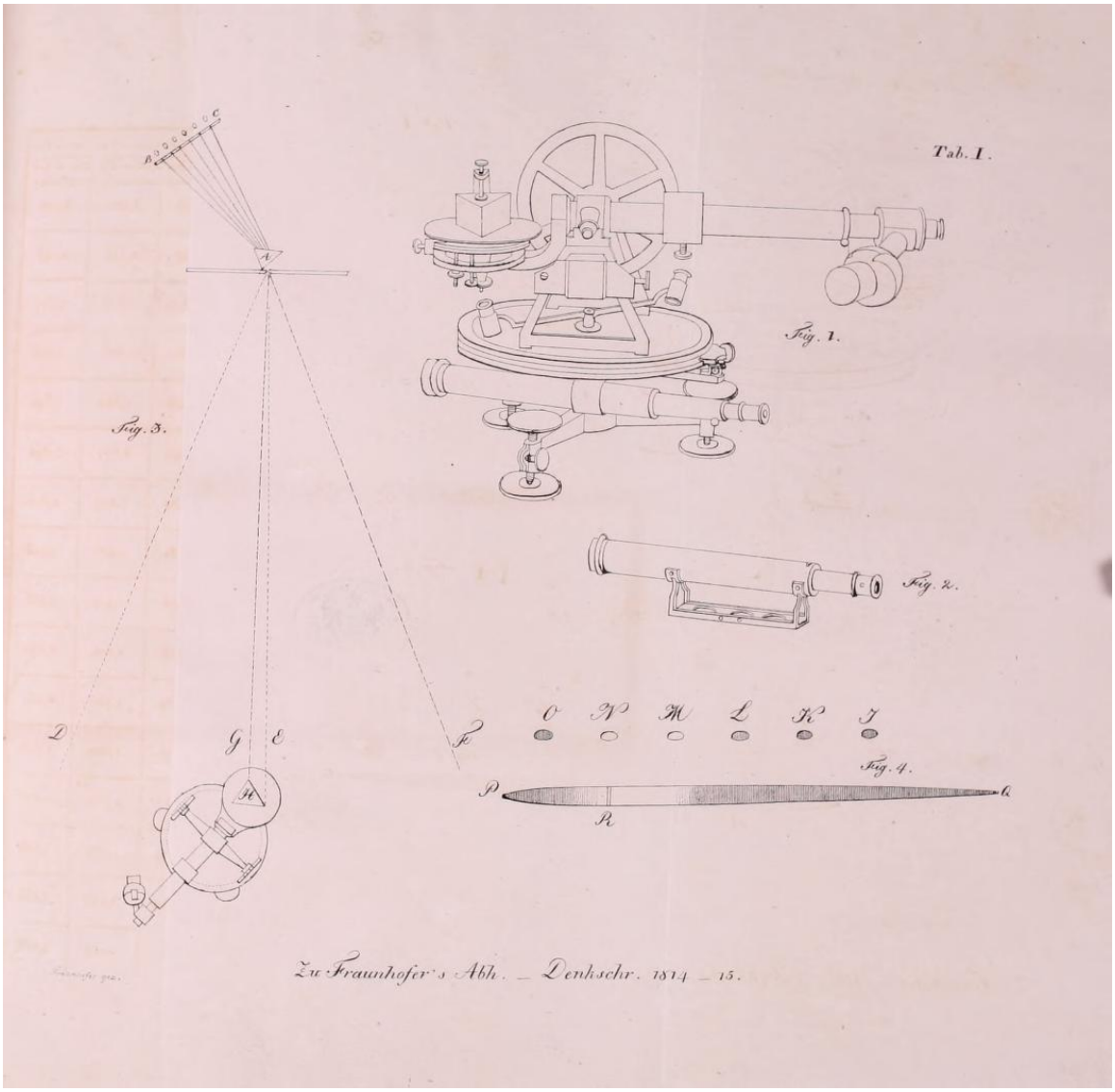


Figure 1.1: Josef von Fraunhofer's instrumentation for measuring the refractive indices of glasses at wavelengths of specific lines in the solar spectrum. [12]


Figure 1.2: Josef von Fraunhofer's rendering of the solar spectrum with dark lines labeled by letters. A continuous spectrum in the background with intensity is shown in the upper graph. [12]

argument in the inverse transform to find the original $h(t)$ without renormalizing the intermediate result.

An atom in isolation absorbs and emits photons for which the photon energies are determined by atomic states of the transition and the energy uncertainty that arises from the finite lifetime or transition probability. With infinite lifetime the spectral distribution is a $\delta$-function about the transition frequency $\nu_0$. In a semiclassical treatment of the physics of emission, the atom is a quantum system that couples to the classical radiation field, and the spectrum that is emitted is given by the Fourier Transform of the time-dependent radiative process. As a consequence of the exponential decay of the radiative amplitude, the spectrum exhibits a distribution of frequencies following a Lorentzian line shape centered on the frequency for the atomic transition for which the width is inversely related to the lifetime $\tau$. Let $\nu_0$ be the atomic transition frequency (usually in Hz), and consider

an exponentially damped oscillator such as

$$h(t) = \exp(-|t|/\tau)\cos(2\pi\nu_0 t) \quad (t > 0) \tag{1.6}$$

where we have chosen to make it a symmetric function of $t$ that is zero for $t < 0$. Its Fourier transform is

$$\begin{aligned} H(\nu) &= \int_{-\infty}^{+\infty} \exp(-|t|/\tau)\cos(2\pi\nu_0 t)\,(\cos(2\pi\nu t) - i\,\sin(2\pi\nu t))\,dt \\ &= \int_{0}^{+\infty} \exp(-|t|/\tau)\cos(2\pi\nu_0 t)\cos(2\pi\nu t)\,dt \end{aligned} \tag{1.7}$$

which is a standard integral that evaluates to a Lorentzian

$$L(\nu) = \frac{1/\tau}{(1/\tau)^2 + 4\pi^2(\nu-\nu_0)^2} r \tag{1.8}$$

$$= (1/2\pi)\cdot\frac{(1/2\pi\tau)}{(1/2\pi\tau)^2 + (\nu-\nu_0)^2} \tag{1.9}$$

The spectral line has a half width at half maximum intensity $\gamma$ given by

$$\gamma_{\rm Hz} = 1/2\pi\tau \tag{1.10}$$

$$\gamma_{\rm rad/s} = 1/\tau \tag{1.11}$$

where care is needed over the possible confusion with widths in frequency (Hz) or angular frequency (radians/second). The area under this Lorentzian integrated over all frequencies $\nu$ is then

$$A = \int_{-\infty}^{+\infty} \frac{1}{\pi\gamma}\cdot\frac{\gamma^2}{\gamma^2 + (\nu-\nu_0)^2}\,d\nu \tag{1.12}$$

$$A = 1 \tag{1.13}$$

The width of the Lorentzian increases when the lifetime decreases.

There are other line broadening effects to deal with too, depending on the source of the radiation. These include

- Doppler broadening due to thermal motions of individual radiating atoms in hot gases
- Doppler broadening due to macroscopic motions of spatially unresolved turbulent or convective sources

- Doppler effects due to rotation (on the width and shape) and translation (on the central frequency)
- Ion collisions (which may be treated with methods similar to those described here, given a potential energy)
- Electron collisions in a plasma (becoming problematic at very high electron and ion densities)
- Extreme density and long-range correlation in liquids and solids, or at very low temperatures

There is currently no completely unified treatment of spectral line formation that accurately includes all these possibilities, or others. Here we focus on the affects of neutral atomic collisions. Doppler effects can usually be incorporated by convolution if the broadening by collisions has a small dependence on temperature. Ion collisions can treated in the same way as neutrals, though historically they are combined with electron broadening for application to plasmas, and the ion interactions treated approximately. This approach fails at high ion density. Electron collisions have been very thoroughly studied and used for plasma diagnostics. The regime of electron densities above $10^{19}$ cm$^{-3}$ remains to be understood well.

## 1.2 Effect of atomic collisions on the spectrum

A simple view of how the environment of a radiating atom affects its spectrum is that any collision interrupts the radiation, abruptly changing its phase and effectively cutting it off. A Poisson distribution of intervals from one collision to another then also leads to a Lorenztian in which the line width is given by the mean time between collisions rather than the lifetime of the state. [1] This idea developed into the conventional one of so-called impact broadening, and ultimately to simplified treatments of collision broadening in which the time between impacts was set by an ad hoc choice of phase change that would have a significant effect on the line width. Before computing hardware and methods were up to the task, atomic physics dealt with the issue by analytical solutions and approximations, often invoking an equally simple view of atomic interactions. One of these approaches, to

use a square well of fixed depth and radius, is exquisitely useful for revealing the basic effects of collisions on the line width, shift, and shape, even though it is not physical. One of the discoveries that came out of the study of neutral atomic spectra affected by noble gases was that far from the line center relative to the width of the impact broadened line the radiation is determined by close collisions, and captures the effects of short duration events. The square well and other analytical techniques aided the development of our understanding of how collisions affect spectral lines. Today line shape measurements are used to inform about atomic interactions, both through the effect of the Boltzmann factor on whether such close collisions are probable, and on finding potential regions where the change in the radiative energy perturbation with distance is stationary. Those regions have enhanced intensity that have been named "satellites" in the line-shape literature, and their dependence on fine detail in atom-atom potentials may be used to validate precise a priori molecular state calculations that can then be employed for a wide range of states not easily accessible to direct confirmation with other methods.

The study of these features has a long history in atomic spectra, and for many years their explanation remained a contentious mystery. By the time of our review of neutral atom non-resonant collisions in 1982, the origin of spectral line collision satellites was largely (but not exclusively) accepted by the community as due to atomic interactions in the region of extrema in the difference potential for the states of the transition of the radiating atom interacting with a single perturber. The comprehensive history, theory, and review of experiments that were done now nearly 40 years ago was presented in a review paper at that time. [1] It highlighted two compelling experiments with analyses that atomic collisions could do more than simply make a line wider and shift its frequency:

- The dependence of satellites on excited state quantum number seen in principle series spectra of alkali atoms [20, 17]
- The discovery of satellites at multiples of the same difference frequency due to multiple-perturber collisions [19]

The first of these revealed remarkably how the spatial region in which the satellite feature developed moved outward from the radiating atom for more highly excited states, correlating the perturbation with the scaling of the atomic wavefunction, and specifically for alkalies with the hydrogenic

atom's size $a_0 n^2$ for increasing $n$. The second validated a useful concept that for long range interactions the effects of two or more perturbers could be treated adequately by adding their individual perturbations on the radiator. As a result, a framework for calculating the complete spectrum of an atom influenced by non-resonant interactions with other atoms was developed that has been applied widely to laboratory sources, and to stars, brown dwarfs, and exoplanet atmospheres. [2] Modern computing methods and vast improvements in computational speed allow the evaluation of line profiles that accurately represent the width, shift and line wings when the composition, density, and temperature of the neutral environment is known, given sufficiently accurate interaction potentials. The difficulty of using this systematically in astrophysics lies in the need for precision in the potentials that exceeds the limits of computational accuracy in complex many-electron systems.

# Chapter 2

# Atomic interaction potential energies for spectral line shape calculations

The interaction potential energies and the transition dipole moment enter into the calculation of a spectral line shape in the time-domain evaluation of the change in the phase of the radiation during a collision. The effects appear in the spectrum after a full duration of collision calculation of the correlation function, and its Fourier Transform.

The spectrum, $I(\Delta\nu)$, is the Fourier transform (FT) of a electric dipole transition autocorrelation function, $\Phi(s)$. For a perturber density $n_p$, we have

$$\Phi(s) = e^{-n_p g(s)} \ , \tag{2.1}$$

where the decay of the autocorrelation function with time leads to atomic line broadening. (See Eq. (121) of [2].) Our approach introduces the concept of a modulated electric dipole transition moment $\tilde{d}_{if}(R(t))$ into the line shape calculation.

$$\tilde{d}_{if}[R(t)] = d_{if}[R(t)]e^{-(V_i[R(t)]/2kT)} \ , \tag{2.2}$$

The potential energy for the initial state is

$$V_i(R) = E_i(R) - E_i^\infty \ . \tag{2.3}$$

and the difference potential energy $\Delta V(R)$ for a transition $i \to f$ is

$$\Delta V(R) = V_{if}(R) = V_f(R) - V_i(R) \ . \tag{2.4}$$

The Boltzmann factor $e^{-(V_i(R)/2kT}$ in Eq. (2.2) appears because the perturbing atoms or ions are in thermal equilibrium with the radiating atom which affects the probability of finding them initially at a given $R$. The electric dipole transition moment taken between the initial and final states of a radiative transition determines the transition probability for a radiating system, which is two atoms in collision. Unlike the case of the isolated atom, the transition probability for a specific pair of states depends on the separation of the two atoms. This modifies relative contributions to the profile from different pairs of the initial and final system states along the collision trajectory, affecting the temporal evolution of the radiation and thereby the spectrum. If electronic states $i$ and $f$ of an isolated radiator are not connected by the electric dipole transition moment operator, that is if $d_{if}(R \to \infty) = 0$, allowed radiative transitions cannot occur between these two states when the interacting atoms are not in collision. Although this transition would not contribute to the unperturbed line profile, $d_{if}(R)$ differs from zero when the neighboring atom passes close to the radiator if the basis states are mixed by the atomic interaction.

With this in mind, what are the requirements for information about the interaction of a radiating atom and a neighboring one colliding with it that are needed to find the shift and shape of the atomic spectral lines of that system? Simply stated these are

- Use justifiable first-principles physics with few if any adjustable parameters
- Have a specific treatment of all states of the atom that are relevant to the observable spectrum: states interact with one another
- For the line wings, provide accurate potentials at short range where the perturbations of the isolated atom correspond to the difference frequency from the line center

- For the line width and shift, even at low density, provide very accurate eigenstate energies ($10^{-4}$ cm$^{-1}$) in the asymptotic approach to infinity
- Produce potentials that have no abrupt non-physical changes that may be from reassignment of states in multi-configuration methods
- Correspond exactly to the isolated atomic states at long range
- Include state mixing to have the variation in transition dipole moment as a function of distance

There are at least three families of potentials in recent use for neutral atom spectral line collision broadening calculations, none of which meet all of these criteria.

## 2.1 Induced dipole van der Waals potentials

The self-energy of two dissimilar atoms includes a dominant contribution from the interaction of the momentary dipole moment of the excited atom with the dipole induced by polarization of the perturbing neighbor atom. The resulting energy change has a dependence on $R^{-6}$, where $R$ is the separation of the atoms. We have known for over 50 years that this convenient description of the interaction is incomplete, and therefore inadequate to provide even approximate values of line widths, or shifts. [1] However, a van der Waals long range attractive interaction leads to a low-frequency wing line shape decreasing as $(\Delta\nu)^{-3/2}$ that has been validated in experiments dating from the early days of analytical atomic spectroscopy. [26][25]. Thus we know that the interaction is an important but incomplete description of the the energy changes occurring in atomic collisions.

The potentials and resulting line widths were introduced into models of stellar atmospheres using reference formulations developed by Unsold [46]. They are still found in stellar atmosphere spectral synthesis code where better data are not available, though based on scaling and modifications that attempt to account for the large inaccuracies of a simple van der Waals potential in modeling spectra from hydrogen- helium- or carbon-rich stellar atmospheres. [15] Many experiments have shown that the van der Waals potential does not work to account for the broadening observed, even in

cases where the ambient gas is highly polarizable and spherically symmetric like the noble gases.[32] [18] Consequently, adjustments to the broadening rate by scaling to bring computed widths into agreement with experiment have no physical basis, though they may be useful for estimates when better methods are not available.

Other alternatives to the van der Waals potentials which behave similarly but account for short range interactions more accurately have been proposed and compared with experiments. A study of line widths, or damping constants, for use in stellar spectra made comparisons with laboratory experiments for the sodium D-lines and found that pseudopotentials were significantly better at explaining dependence on temperature.[32] An analytical potential based on the van der Waals concept that behaves as $R^{-6}$ at long range but is finite and suitable for computation at shorter range was developed to use parameters refined by comparison to experiments.[17] Lwin and McCartan found that this approach worked well in all the cases they had tested for the alkali atoms broadened by noble gases.[30] Nevertheless, broadening in a stellar atmosphere with atomic hydrogen as the environmental gas for spectral lines of sodium, potassium, calcium, magnesium, and iron that are important diagnostic lines for stellar spectra cannot be validated in the laboratory under the same conditions that are present in stars. Noble gases such as xenon become a proxy for hydrogen, and even then the comparisons are done at lower temperature and the dependence of broadening on temperature has to be understood to extrapolate to stellar conditions. Contemporary models of stellar atmospheres make use of various sources for the line broadening coefficients weighing the accuracy and comprehensive availability of needed atomic data.[13][9][22]

## 2.2 Ab initio molecular potentials

The basic principles of many-electron systems with two centers are understood, and the quantum mechanical solutions of the energy eigenstates could be found for any atomic separation in principle. There are well-maintained codes to this end and a user community supporting their use. [49] Many of these, Molpro perhaps the most widely used commercial one, are optimized for large molecules and for solid state. [48] Others are intended to study basic physics in smaller systems with Hartree-Fock methods, of which Dirac is an open source example. [43] There are few examples of ab initio calcula-

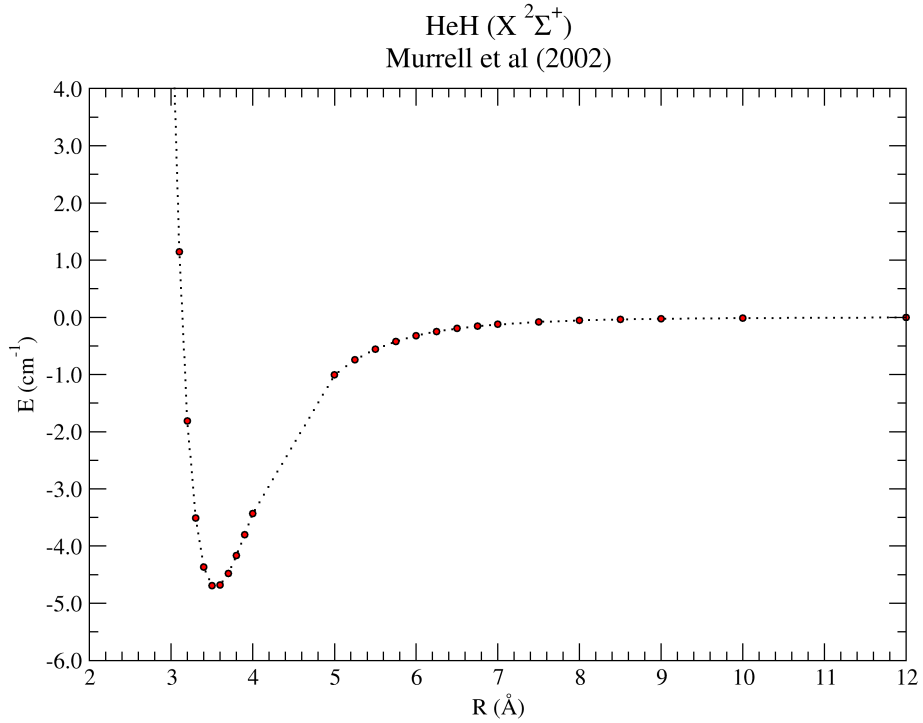


Figure 2.1: The ground state of HHe from the Molpro ab initio calculation of Murrell et al using an RCCSD(T)/EVEN-2 basis set. [34] The uncertainty in the well depth is $\pm 0.3$ cm$^{-1}$. The data extend to 20 Å where the perturbation from the asymptotic atomic state is 0.0002 cm$^{-1}$.

tions taken from the asymptotic limit of infinite separation into the regime of close collisions where radiative events are improbable.

One of the simplest neutral systems beyond $H_2$ is H-He with three electrons and two positive charge centers. H-He as a molecule has been studied often, and still remains a challenge even with the most recent ab initio codes and techniques. An example is the study by Warnecke et al. in which analytical methods of Tang and Toennis were compared to the best ab initio calculations published at that time for the lowest state $^2\Sigma^+$ state. [45][47]

They found agreement with the latest ab initio potentials over six orders of magnitude that is comparable to the differences in the available ab initio

H-He calculations. One of these was a Molpro computation by Murrell et al (2002) using a RCCSD(T) procedure that the authors say is for open shell instances when multi-reference configuration interaction (MRCI) behavior is small. [34] They noted that MRCI calculations are computationally expensive and limit the size of the basis set, while also requiring judgement on which basis states to use. Their choice was made to achieve efficiency and they showed that it gave the same potential as a previous full configuration-interaction calculation using the same basis set they chose. The result is shown in Fig. 2.1 They obtained a depth of the X $^2\Sigma^+$ ground state well at $R_e = 3.548$ Å of $D_e = 4.720$ cm$^{-1}$ with variance $\pm 0.3$ cm$^{-3}$. The need in line shape calculations is for absolute accuracy of 1 part in $10^3$ in the region of the potential minimum, and $10^{-4}$ cm$^{-1}$ asymptotically in order to compute a spectrum that is directly comparable with observation without adjustment. Their results for the ground state nearly meet that target. In the H-He system other states of interest for atomic spectra are the limited subset for which the H atom is excited while the He atom is not, that is the Balmer and Lyman series of atomic H broadened by He. In those instances, the H electron is far from the nucleus, and the system is treatable with the proton, electron and He atom as distinct components where is far from the hydrogenic proton and retains its identity. The methods and results of Warnecke et al, and Murrell et al would still apply at least as a guide to the relevant physics and appropriate numerical methods. At this time there are no published calculations of the potential energies and dipole transition moments for one-electron excitations of H-He.

.

## 2.3 Analytical methods and effective potentials

Fundamentally, evaluation of the potential for a two-atom system could be treated as a many-body problem with all of the atom's electrons and two nuclei to find the eigen-energies and states of the system. We conceptually isolate this pair of atoms from the rest of the universe, and in the case of H-He have 3 electrons and two positive nuclei of different charges. This problem has only been solved exactly in the two limiting cases of infinite separation into two isolated atoms and merger into a lithium atom. Indeed,

even in those cases the details of the solution are still challenging because of the Lamb shift, the contact terms in hyperfine structure, and multi-electron correlation. On the other hand, we know experimentally the energies of the isolated atomic states and a set of quantum numbers that largely describe those states well. We can leverage this knowledge, and the physics where the electrons of both atoms are tightly bound to their nuclei excepting the valence electron of one atom, to separate the Hamiltonian into two parts: the energy of the ambient unexcited atom that remains unchanged, and the energy of the perturbed atom with its valence electron. The Hamiltonian of this system has terms for each atom in isolation and an effective interaction term representing the contribution of the valence electron of atom A interacting with atom B, and the entirety of atom B interacting with the core of atom A. The term "effective potential" theory is sometimes used to identify this approach, and it divides into two alternative methods that are more widely known as "model-" and "pseudo-" potentials which may be confused with one another in practice. Inevitably, solutions for the potential energies for the interaction of one and two electron atoms (e.g. H, Na, Ca, Mg ...) with unexcited monatomic gases (He, Ne, Ar ...) approached this way have some parameters that must be found by comparison to experiments or precise ad hoc potentials. When successful, the results can be as good as the ad hoc calculations and extensible at low computational cost. Even in non-ideal situations where the parameters are not optimized or the effective potential is incomplete, they offer qualitative guidance on the potentials as a function of atomic separation and transition probabilities.

Pseudopotentials as a method of calculating atomic and molecular structure are now widely used, and perhaps equally widely misunderstood. It is not only the confusion of terms we have seen in the line shape literature, but what the methods mean, and whether they can be exact. Light on this topic is offered in the work of Levente Szasz, with an informative but little-known book.[44] The main point made there is that in general pseudopotentials are simply a way of representing the Pauli exclusion principle by an operator which can be evaluated in an appropriate set of basis states.

Masnou-Seeuws considered the use of these methods for alkali- and alkaline- atom states affected by noble gases. and drew a distinction between model- and pseudopotentials in their treatment of the interaction of the valence electron with the noble gas atom, and of the noble gas atom with the atomic core of the alkali atom. [31] We begin with two atoms, one of which has a valence electron that has a high probability of being far from

the nucleus compared to extent of the core and the separation of the atoms. The other atom is so tightly localized that it is treated as a single object with a constant internal energy. The total energy of the system is the sum of the energies of the two atoms, where the contribution from A depends on the separation of the atoms $R$ while the contribution from B is constant. We find the energy of the system relative to the separated components of the core of A, the electron, and the intact atom B, assuming that the atoms are at rest with respect to one another and ignoring the internal structure of B which typically will have energy states far above those of interest in A. In the Born-Oppenheimer approximation the nuclei are fixed, separated by $R$, and the Hamiltonian has three terms arising from the kinetic energy of the electron $T$ in the center-of-mass system with its parent nucleus, and its interaction with the core of its parent A ($V_A$) and with the entire atom B ($V_B$),

$$H = T + V_A(r_A) + V_B(r_B) + V_P(R, r_A, r_B) \tag{2.5}$$

There is a fourth electron polarization term $V_P$ that includes the interactions of the electron and the core of A with the instantaneous dipole moment induced in the atom B. This term is obviously complex, depending on 3 bodies and the angles, and the electric dipole polarizability of the atom B that is taken as a given value rather than computed ad hoc. At large distances where the electron is most probably close to its nucleus this term includes the dipole–induced-dipole van der Waals interaction. At smaller distances it has quadrupole moment interactions and increasingly significant short range interactions.

The basis states for computing the potential with this Hamiltonian are the complete set of states for the atom A with $R$ at infinity. Pseudopotentials are computed in framework built on the idea of the quantum defect method in which these states and the interaction of the electron with its core have the correct behavior where the electron is outside the core of A, while inside A they have no nodes and are the hydrogen-like states that give the observed energies for the alkali. The radial wavefunction is given by an effective principle quantum number $n^\star$ and angular part by the usual basis set that may be $|(LS)JM>$ if spin-orbit interactions are included. Alternatively, the wavefunctions have the correct number of nodes at small $r$ also with the same behavior outside the core of A. Model-potentials are computed in this framework. For long range interactions where $R$ keeps the

atom B outside of the core of A, the two methods should yield the same result. They are formally identical in the case where A is a hydrogen atom.

As Masnou-Seeuws points out, the treatment of $V_A$ can enable matching observed behavior of the atomic states in isolation (i.e. where $R$ is neglected) to refine the wavefunctions. One can also assume a form of the wavefunction that reproduces the known atomic states, as in the pseudopotential method, and thereby have some $\ell$-dependence without the computational overhead. Prior to our review in 1982, there were several key papers advancing these ideas and applying them to spectral line broadening. [1] To highlight a few, consider the landmark paper by Baylis [6] and those that followed

**Baylis (1969)** introduced the idea of a simple semi-empirical method for evaluating semi-empirical pseudopotentials for use in spectral line broadening. [6] The parameters of the model could be adjusted to match then known potentials and experimental data.

**Pascale and Vandeplanque (1974)** used the method of Baylis with a large number of atomic states and showed that coupling among the molecular states was important and the cause of structure in the excited state potential curves. [39][37] The work led to comprehensive tables of potentials for the lower electronic states of alkali atoms perturbed by noble gases that were distributed but unpublished. pseudopotentials with $\ell$-dependent operators were developed later and published for alkali-helium systems. [38]

**Czuchaj and Sienkiewicz (1974)** repeated the work of Baylis [6] with a different wavefunction and treatment of core-core term. They found similar results to the Pascale and Vandeplanque potentials as well as discrepancies. [8]

More recently, work on effective potentials continued with specific case studies and added detail in treatment of the core interaction terms. Highlights are

**Masnou-Seeuws (1985)** review as noted above says that many accurate properties of systems with one active electron have been obtained, and notes the need to treat core polarization. [31]

**Szasz (1985)** wrote a book on the use of pseudopotentials in atomic and molecular physics in which the validity of the method was explained, and its relationship to ab initio calculations done in other ways explored. [44] The book did not discuss line broadening, or the work of Baylis and others familiar to the line shape community. It demonstrated perhaps a disconnect between those engaged in the spectral line shape problem, and those working on fundamental solutions to precise atomic and molecular computation.

**McCartan and Lobb (1990)** make a comparison of sodium line broadening experiments and computed spectral line profiles from available potentials. By consistently using the same line shape theory of Lewis and McNamara [28] for the line core width and shift and potentials from many different sources, they conclude that available potentials are "not universally applicable." Of particular note is that potentials that describe the line wing may be inadequate to predict the broadening and shift of the line core. The pseudopotentials of Pasquale and Vandeplanque [39] were the most successful, and the simple analytical potentials of Kielkopf [17] provided the most consistent set of published data. They noted critically that the increasingly sophisticated potentials since then did not improve predictions of line shift and width.

**Partridge et al (1993)** with MRCI ab initio calculations of H-He and other rare-gas hydrides find agreement with analytical and pseudopotentials. [36]

**Dickinson and Gadéa (2002)** study Li-He using the Fermi model for the contact interaction. They show it yields physically sound excited state potentials and a deep understanding of the unusual shapes of the adiabatic curves. [10]

**Peach (2010)** considers potentials for broadening of spectral lines of astrophysical interest, particular cool dwarf stars where alkali atom lines broadened by H and He are observed. She tests the validity of van der Waals models against detailed quantum mechanical calculations to show that van der Waals potentials significantly underestimate line widths. She concludes that the van der Waals potentials are inade-

> quate for the analysis of astronomical spectra and that significant errors arise from their use. [40]

After more than 50 years of development since the era of computational physics, the state of the art in predicting the core width and shift and the wings of atomic lines broadened by atom and ion collisions remains limited by the lack of interaction potentials that include all the states, and span the range of atomic separations with the precision required to compute a line profile. The summary of Lobb and McCartan still is true that available potentials are not adequate to the task.

# Chapter 3

# A useful simple pseudopotential

## 3.1 Justification

The Pascale and Vandeplanque potential in its simplest form, computed with a large number of basis states, remains a benchmark result with sound physical basis. [39] It is also clear from the many experiments, other effective potential calculations, and ab initio potentials that the parameterization of pseudopotentials is a critical factor in determining whether they will be successful, and that potentials developed to model one region of the spectrum may not be the best ones for another region. Several years after the community effort to find best practices to determine spectral line shapes from first principles, Lobb and McCartan made the retrospective observation that efforts with increasing complexity were not improving the agreement with experiment. [29] They noted that the Pascale and Vandeplanque approach had the best outcome, and apart from a few successes with ab initio potentials, there has been little to change that viewpoint today. Therefore, we review a potential proposed by Allard and Kielkopf [1] which derived from the formulation of Pascale and Vandeplanque, has the simplicity and uniformity that allows evaluation over a very wide range of atomic separations, and invokes a small number of parameters to enable a simple predictive capability when adjusted to either physically based estimates or fitted values.

## 3.2 Underpinning physics

As with other calculations of this type, the model proposed here is based on sound physics, but has parameters that have to be adjusted to achieve results that are reasonably comparable with experiments when the perturbations of the radiating atom are "large", that is when the perturbing noble gas atom is inside the mean radius of the radiator's electron probability distribution. Nevertheless, at very large range the methods are essentially exact, apart from retardation and in our implementation the absence of the quadrupole moment term. Even without tuned parameters, the potentials provide insight into the behavior at long range, and critically the mixing of atomic states caused by the dipole interaction. This method avoids a pitfall of the Baylis pseudopotential which attempts a more exacting calculation of the contact interaction of the valence electrons with the perturber. In that approach, parameters must precisely balance large attractive and repulsive contributions and the sum is extremely sensitive to the choices. We take a simpler concept of the physics of the electron-noble gas contact interaction, invoke the now-conventional ideas of Gombas, and use estimates of parameters that have easily visualized physical meaning. The results agree qualitatively with a priori models that are currently available.

The following explanation of the potential calculation is from Allard and Kielkopf [1] with changes reflecting the current program. The Fortran code implementing this potential is open source and available on line.

## 3.3 Basis states

The calculations are done in an atomic basis set representing the isolated atom with valence electrons. The other atom, presumably a tightly bound perturber such as a noble gas atom, is assumed spherical and unexcited. Its wavefunction explicitly enters only in one term of the interaction which to first order is the same for all states of the atom that are of spectroscopic interest. The effect of this choice is that the asymptotic energy levels will agree precisely with experiment if the wavefunctions are chosen to reproduce the free atomic energy levels. The basis set is $|n\ell(SL)JM>$ determined by the principle quantum number $n$ and orbital angluar momentum $\ell$ of the valence electron in the case of an alkali atom, the total orbital angular momentum $L$, total spin $S$, and the coupled total angular momentum $J$

with its projection on the z-axis $M$. LS coupling is used as is conventional for the alkali and alkaline earth elements. The asymptotic states are almost purely these basis states, and selection rules apply rigorously with few if any intercombination or forbidden transitions having significant line strength. This choice therefore also greatly simplifies calculating the transition dipole moments of the resultant molecular states.

The value of $M$ is a good quantum number for each molecular state when the levels are split by the interaction with other atom, and there is no difference in energy between the two states $\pm M$. The specification of $|M|$ and the parent atomic state of the alkali identify each eigenstate at any $R$. When the spin-orbit interaction is neglected the projection of $L$ on the internuclear axis gives $M_L$ and allows states to be labeled uniquely by $\Sigma$, $\Pi$, $\Delta$ and so on, corresponding to $M_L = 0$, $\pm 1$, and $\pm 2$, also degenerate in the sign of $M_L$. However alkali fine structure is important even for hydrogen, and such labels are not good quantum numbers, that is, the actual states are mixed, and the degree of mixing of the relative contributions of the basis states depends on $R$. This has significant implications for the interpretation of potential energy curves. For example, an excited atomic $p$ state gives rise to a $\Sigma$ and a $\Pi$ molecular state. The $\Sigma$ state is repulsive at long range because there is a lobe of the probability distribution of the valence electron along the internuclear axis. The $\Pi$ state has less repulsion and may be attractive at long range because the perturbing rare gas atom does not encounter the alkali valence electron which is most probably near a plane perpendicular to the axis. The parentage of these states determines the transition probability, and is affected significantly by the selection rule that $s \rightarrow s$ transitions are forbidden for electric dipole radiation.

## 3.4 Contributing terms

To enable the calculation, the basis $|n\ell(SL)JM>$ is expanded in terms of the one-electron states $|n\ell m_\ell s m_s>$ in which we calculate matrix elements of an effective Hamiltonian that is added to the Hamiltonian of the atoms in the system.

$$H_{\text{interaction}} = F(\vec{r}, \vec{R}) + G(\vec{r}, \vec{R}) + W(R) \tag{3.1}$$

The vectorial character of the separation of the electron ($\vec{r}$) and the perturbing atom ($\vec{R}$) from the radiating atom is explicit in F and G. The function F

is the interaction of the valence electron and the ion core of the alkali with the dipole moment of the noble gas they induce. G is a pseudopotential representing the so-called Pauli exclusion pressure that keeps the valence electron out of the space occupied by the noble gas electrons. W is the interaction of the core of the alkali or the hydrogen nucleus proton with the noble gas. Each is a consequence of the presence of the noble gas atom in the vicinity of the radiating atom, and especially its valence electrons. These terms asymptotically approach zero at infinite $R$, leaving only the atomic state energies. We consider them individually.

## Induced dipole interactions

We calculate the interaction of the atom with an unexcited, spherically symmetric perturbing atom of known polarizability using electrostatic expressions for the interaction $V(R)$. This depends on the vectors $\vec{R}$ from the atom core to the perturber, and $\vec{r'}$ from the perturber to the valence electron.

$$< V(R) > \;=\; -\frac{1}{2}\alpha < \vec{E}(\vec{R})^2 > \tag{3.2}$$

$$\vec{E} \;=\; e\left(\frac{\vec{R}}{R^3} + \frac{\vec{r'}}{r'^3}\right) \tag{3.3}$$

where $\vec{E}(\vec{R})$ is the total electric field at the perturber atom due to both the valence electron and its core. The dipole polarizability of the perturber $\alpha$ is taken as a known quantity representing the response of the perturber to an external field. Therefore the valence electron and the nuclear charge center must be excluded from the volume occupied by the perturber when evaluating Eqs. 3.2 and 3.3, and within that volume, some other solution must apply. We let $\Theta(r' - r_0)$ be a step function that is one when $r' \geq r_0$ and zero inside $r_0$, and identify a parameter $r_0$ to represent the radius of the perturber. The contribution to the dipole interaction term when the electron and the atom's positive core are outside the perturber is then exactly

$$F \;=\; -\frac{\alpha e^2}{2R^4}(1 + 2rR^2r'^{-3}\xi - 2R^3r'^{-3} + R^4r'^{-4})\,\Theta(r' - r_0) \tag{3.4}$$

$$\xi \;=\; \cos(\vec{r}, \vec{R}) \tag{3.5}$$

Baylis [6] showed that the function $\Theta$ could be expressed as an expansion in Legendre polynomials

$$r'^{2q}\,\Theta(r'-r_0)=\sum_{\ell=0}^{\infty} f_q^{(\ell)}\,P_\ell(\xi) \tag{3.6}$$

The first two coefficients $f_q^{(0)}$ and $f_q^{(1)}$ are analytic integrals

$$f_q^{(0)} = \frac{1}{2}\int_{-1}^{\xi_0} d\xi\,(r^2+R^2-2rR\xi)^q \tag{3.7}$$

$$f_q^{(1)} = \frac{3}{2}\int_{-1}^{\xi_0} \xi d\xi\,(r^2+R^2-2rR\xi)^q \tag{3.8}$$

evaluated explicitly with special functions. From them we use a recursion relation

$$\begin{aligned}\chi f_q^{(\ell)} &= \frac{r_0^{21+2}}{4rR}\left[P_{\ell+1}(\xi_0)-P_{\ell-1}(\xi_0)\right]\\ &+ \frac{q+\ell+2}{2\ell+3}\,f_q^{(\ell+1)}\\ &+ \frac{\ell-q-1}{2\ell-1}\,f_q^{(\ell-1)}\end{aligned} \tag{3.9}$$

to find any higher $f_q^{(\ell)}$ where $\chi=\cos(\vec{r},\vec{R})$ for $r'=r_0$

$$\chi=(r^2+R^2)/2rR \tag{3.10}$$

This contribution to the induced dipole potential from $r'>r_0$ and $R>r_0$ is given by a sum over Legendre polynomials in $\xi$ with coefficients $F_\ell(r,R)$

$$F=\sum_{\ell=0}^{\infty} F_\ell(r,R)\,P_\ell(\xi) \tag{3.11}$$

The terms of the expansion are then

$$F_\ell=-\frac{\alpha e^2}{2R^4}\times$$

$$\left(f_0^\ell-2R^3 f_{-3/2}^{(\ell)}+R^4 f_{-2}^{(\ell)}+2rR^2\left(\frac{\ell}{2\ell-1}f_{-3/2}^{(\ell-1)}+\frac{\ell+2}{2\ell+3}f_{-3/2}^{(\ell+1)}\right)\right) \tag{3.12}$$

When $R>r_0$ Eq. 3.12 is valid for all $r$ and will give zero when $r'<r_0$.

The improbable but significant contact interaction with $r'$ (or $R$) inside the noble gas atom's cutoff $r_0$ must be handled differently. The step expansion in Eq. 3.6 affords a consistent way to treat that case by adding a term in $(1-\Theta(r'-r_0))$ that is zero outside $r_0$ and 1 inside, using the same expansion in $P_\ell$. Here, we set the polarization contribution to zero and add back a contribution representing a Gombas repulsive contact pseudopotential in $G$. In this way the parameter $r_0$ controls a balance between contributions from the attractive induced dipole and repulsive exclusion principle that can be adjusted to match a priori calculations or empirical data.

## Exclusion principle effects

In an exact a priori calculation the wavefunctions of the noble gas electrons would be part of the system, and the valence electrons as well as the alkali core electrons would see them explicitly. Since the noble gas atom has all its electrons tightly bound in filled $n\ell$ configurations, electrons from the alkali will be excluded due to the Pauli principle. Qualitatively, that is, there is an effective potential energy from the hole in the valence electron probability distribution created by the perturber that raises the system energy, i.e. repels the electron. We use a simple first order representation of this potential based on a method discovered by Gombas that adds a term dependent on the noble gas atom charge density. [14] An equivalent alternative would be to use a scattering length parameter following the work of Fermi which connects these potentials to the scattering of electrons by noble gas atoms and is widely used to explain the behavior of the the line shift of high members of the alkali principle series.[11] [27] These methods are equivalent in this use and the success of both in other applications justifies their use here to simplify the pseudopotentials with an easily adjusted parameter.

The Gombas contact term operator (see [1]) for the valence electron, using an average over the volume within $r_0$ when $r' < r_0$, is [1])

$$G(R) = \frac{\hbar^2}{2m}(3\pi^2)^{2/3}\rho_p^{2/3} \tag{3.13}$$

where $\rho_p$ is the perturber's electron density inside the volume included within $r_0$. More simply in atomic units

$$G(R) = \frac{1}{2}(3\pi^2\rho_p)^{2/3} \tag{3.14}$$

and

$$\rho_p = N_p \frac{3r_0^3}{4\pi} \tag{3.15}$$

$N_p$ is the number of perturber electrons effective in scattering the valence electron. For computational purposes it is convenient to include $G(R)$ with an expansion in $P_\ell$ as

$$G_\ell = g_p \frac{N_p^{2/3}}{r_0^2} \left(1 - \delta_{\ell,0}\, f_0^{(\ell)}\right) \tag{3.16}$$

$$g_p = 1.8415843 \tag{3.17}$$

In this expression both parameters $N_p$ and $r_0$ should be of the order of unity for a He perturbing atom. This positive contribution to the energy acts only when the electron is inside $r_0$.

## Core interactions

Lastly, we have considered the effect of the net charge of the alkali core on polarization of the noble gas up to the point that the nucleus of the alkali is so close that it is inside the noble gas. That would be a separation of the order of the radius $r_0$ which will be typically the scale of 1 Å. The idea is incomplete in two ways. Important even for H interacting with a compact noble gas atom like He, the noble gas wave function extends beyond $r_0$ while decreasing in probability, that is, the cut off is fuzzy. In atoms other than H, the alkali core has a charged center surrounded by a noble-gas-like cloud of filled-shell electrons. The minimalist case of Li-He has the perturbing He atom finding a He-like core once it has passed by the valence electron region of most probability. That is for Li-He there would be a component to the potential analogous to He-He at close range, and similarly for Na-He there would be an Ar-He like interaction from the core of Na with the perturbing He.

Treating the details of these interactions with accuracy is beyond the scope of the simple pseudopotential model proposed here, and is not necessary for using pseudopotentials for line shapes and for understanding long range interactions at least as an adjunct to ab initio calculations. The core-core interactions to first order affect all valence states of the system similarly, and therefore in radiative transitions their effects disappear from

the difference energy that determines the photon's frequency. Thus what would be useful to know is the difference in core-core interactions for various valence states. An understanding of that would be informed by case studies of ab initio models that are validated by experiments. Another affect of the core interaction terms is at close range the high energy barriers they raise affect collision dynamics. They enter into line shape calculations through the Boltzmann factor. For that purpose, extreme accuracy of the sort we seek at longer range is not needed, and estimates based on fitting ground state potentials from ab initio calculations could be used for the dynamics if added equally to all states so that the difference potential is unaffected. The behavior of atomic wavefunctions inevitably takes the form of an exponential dependence on the coordinates of the electrons, leading to a probability distribution that has exponential character at long range. This has been extensively studied in the context of electron scattering, and there are simple analytical wavefunctions that have the correct behavior. [16] [5] [4] These wavefunctions share an exponential decay outside the core and as we expect would lead to a small and decreasing significance of core interactions for spectra of excited states.

For Na-He potentials Pascale and Vandeplanque propose a exponential short range core interaction term in addition to the dipole polarization terms we have discussed in Section 3.4 [37]

$$W(R) = w_C \exp(-(R/R_C)) \tag{3.18}$$

They fit ab initio potentials of $Na^+$-He to find coefficients of the core terms $w_C = 52.681$ and $R_C = 0.402$ in atomic units for Na-He. This potential arises from the core electrons of the alkali and the closed shell electrons of the noble gas atom. Its exponential character presumably derives from the exponential decrease of the electron density of both the alkali core and the noble gas atom with distance from their centers. In the case of atomic H interacting with another atom, there are no core electrons as there are in the H-like alkalies. Still, there would be effects on the interaction from the distant encounter of the proton with the outer part of the noble gas electron density that would have the same character, in first order proportional to the exponentially dependent separation from the noble gas perturber. In treating the noble gas atom as a sphere with fixed charge density for computing $F$ and $G$ we ignore these effects, while the $W$ term can compensate for details that are not in a simple model of an unexcited

polarizable sphere for the noble gas atom. The parameters of $W(R)$, if it is included, may found by comparison to a priori calculations of hydride potentials.

## 3.5 Parameters

The simple pseudopotential described here can be calculated with estimated parameters to obtain representative behavior of an atom with valence electrons interacting with an unexcited perturber. The parameters needed are

**Energy levels** of the states of the atom with a valence electron. These should be sufficiently accurate to predict the observed unbroadened spectrum.

**State classifications** for the valence electron's energy levels, given in a $n\ell(SL)JM$ basis. These classifications are available for all the alkali and alkaline earth one-electron excitations based on spectroscopic and theoretical analysis.

**Dipole polarizability** of the noble gas $\alpha$ or other perturber. Values are known from theory and experiment to a few parts per thousand.

**Cutoff radius** of the noble gas $r_0$ inside of which a Gombas pseudopotential replaces the dipole polarization interaction. This ad hoc parameter, of the order of 1 bohr or an atomic unit of distance for small perturbers, is found by comparison to experiments and a priori calculations to improve the accuracy of the pseudopotentials. It may be estimated from the polarization of a conducting volume of charge $\alpha = 4\pi\epsilon_0\, r_0^3$ in SI units, for consistency with the polarizability of the noble gas atom. [41] For He with a polarizability of $\alpha = 0.205$ Å$^3$ (cgs), this would estimate $r_0 = 0.590$ Å.

**Noble gas core charge** $N_p$ electrons participating in the Gombas pseudopotential for exchange interaction with the noble gas atom. Since noble gases other than He have a filled p-shell, an estimate of $N_p = 6$ for atoms other than He, and $N_p = 2$ for He would be a reasonable prior choice in fitting pseudopotentials to a priori references.

**Core-core** parameters $w_C$ and $R_C$. If used in the simple pseudopotential model, these parameters add an energy to all eigenstates of the system from the core-core interaction. They should be considered if an a priori ground state calculation is used to fit the other parameters for test states since the effect would be common to all states of the system. The expectation is that $w_C$ is of the order of 1 atomic unit of energy ($2E_{\text{Rydberg}}$), and that $R_C$ is of the order of $r_0$ for self-consistency with our cutoff model.

# Chapter 4

# H-He excited state mixing at long range

We have computed the potentials for the states of H-He arising asymptotically from the $1s$, $2s$, $2p$, $3s$, $3p$, and $3d$ states in an atomic $|n\ell(SL)JM>$ basis with Bates-Damgaard wavefunctions and asymptotic energies matching the archival atomic energy level tables for H that include experimental excited state fine structure, but not hyperfine structure or isotope shifts. The parameters used for the calculation are those given in Section3.5 and are notably based on the physics. The results for the ground state where we have an ab initio potential as a benchmark are shown in Fig. 4.1.

As expected, without a term in $W_C(R)$ the pseudopotential is too attractive at small $R$ while still having the correct asymptotic behavior. As described in Section 3.4, the difference is possibly due to the assumption in the model of an unperturbed conducting sphere for the the noble gas. This is remedied by adding for the core interaction for the ground state a term in which the energy scaling is fixed at 1 atomic unit and the radial scaling is adjusted to optimize the match with the a priori potential.

$$W(R) = w_C \exp(-(R/R_C)) \tag{4.1}$$

$$w_C = 2 \times E_{\text{Rydberg}} \tag{4.2}$$

$$R_C = 0.344\ A \tag{4.3}$$

The agreement for $X\,^2\Sigma$ shown is achieved by fitting $R_C$ so that the innermost repulsive wall is aligned with the a priori potential. The resulting

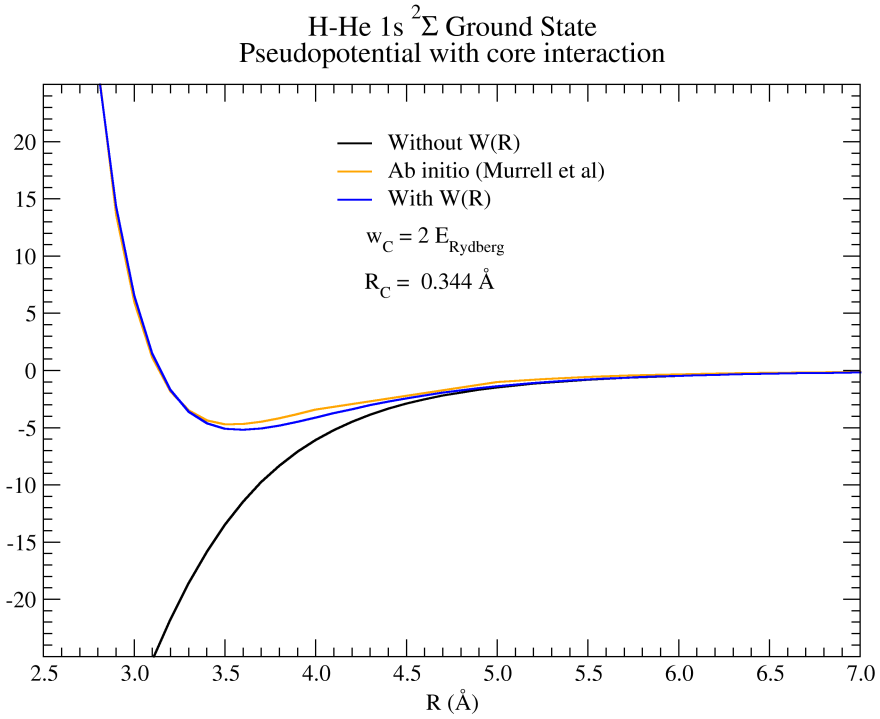


Figure 4.1: The ground state of an H-He pseudopotential calculation (see text) compared to the Molpro ab initio calculation of Murrell et al using an RCCSD(T)/EVEN-2 basis set. [34] A core-core term is necessary to reproduce the ab initio ground state.

ground state well is at $R_e = 3.6$ Å and $D_e = -5.2$ cm$^{-1}$. This compares favorably with the a priori potential's $R_e = 3.55$ Å and $D_e = -4.7$ cm$^{-1}$, lending confidence to the utility of this simplified pseudopotential method.

Recently, Allard et al have developed another Molpro ab initio calculation that reproduces the result of Murrell and includes the states that have $n = 2$ atomic H as asymtotic parents. [3] Figure 4.1 illustrates how the ground date ab initio calculation differs only slightly from the previous one, actually improving the agreement with the ground state potential well of the pseudopotential. It is important to note that this well is due to van der

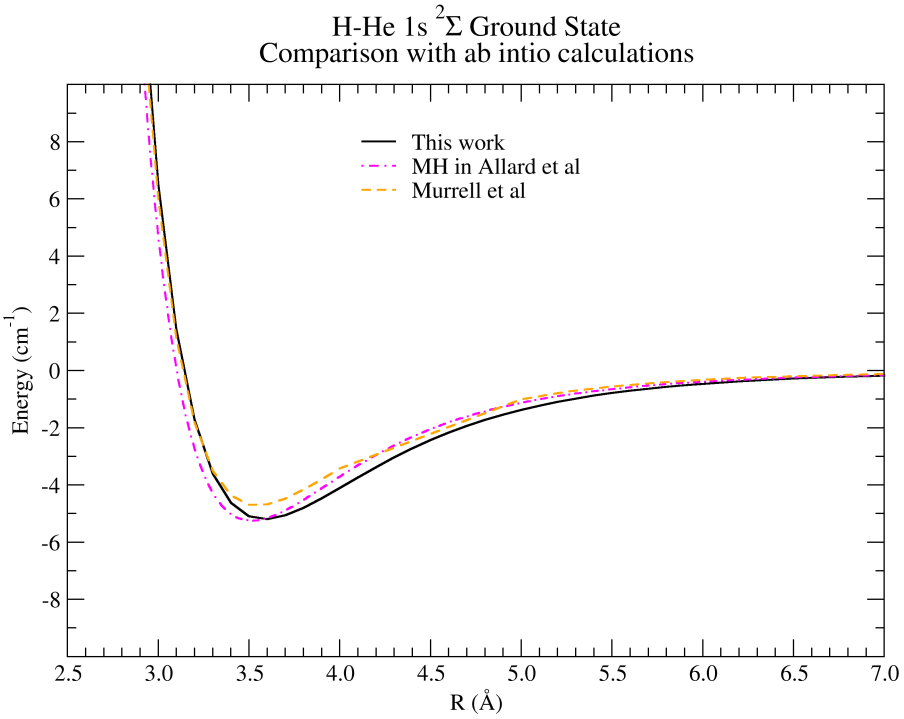


Figure 4.2: The $X\ 1s\,^2\Sigma$ ground state of the H-He pseudopotential calculation (see text) compared to the Molpro ab initio calculations of Allard et al [3] and Murrell [34]. A two-parameter core-core term $W(R)$ is included.

Waals interactions at long range compared to the atomic $1s$ ground state wavefunction since 3.5 Å is far outside the Bohr radius of the atom. At the same separation in the first excited state for $n = 2$ we find a complex set of potential curves which have mixed parentage with the expected behavior of $\Sigma$ and $\Pi$ states. A comparison for the excited state, the upper state of Lyman-$\alpha$, is shown in Fig. 4.3

The pseudopotential calculations are done with basis set complete through $n = 3$. There is one $1s$ state which is degenerate in the sign of $1s$ $L = 0; J = 1/2$ $M_J = \pm 1/2$. Similarly there are 4 states in $n = 2$ which asymptotically go to the experimentally known $2s\ ^2S_{1/2} M_J = \pm 1/2$ "s" state, and

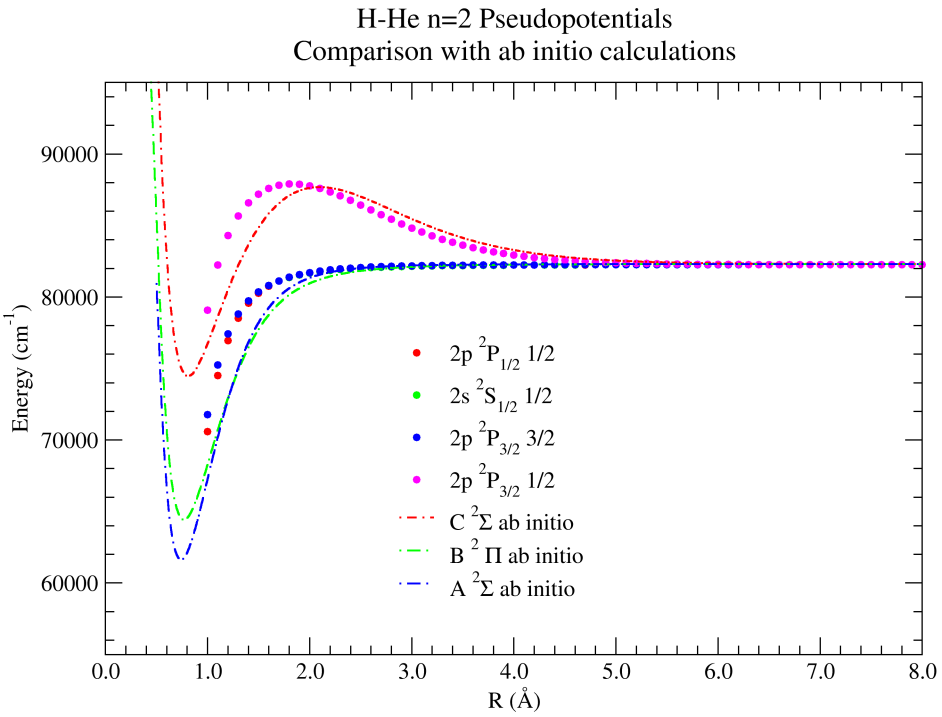


Figure 4.3: The $n = 2$ excited states of an H-He pseudopotential calculation (see text) compared to the Molpro ab initio calculation of Allard et al. [3] The potentials shown do not have a core-core term and were computed with physically reasonable assumed parameters without fitting.

the three "p" states designated $2p\ ^2P_{1/2}\ M_j = \pm 1/2$, $2p\ ^2P_{3/2}\ M_j = \pm 1/2$, and $2p\ ^2P_{3/2}\ M_j = \pm 3/2$. $J$ and $|M_J|$ are good quantum numbers in this basis, and the interaction mixes states of different $L$. In the potential calculation the unperturbed states are assigned the energies given in Table 4.1. The contemporary best values for these levels differ from those in the older literature largely in an improved value for the energy of the $1s - 2s$ two photon transition from laboratory experiments that did not affect the relative energies of the levels in $n = 2$ significantly for comparisons with the literature.

Figure 4.3 shows that the pseudopotential energies and the ab initio

| $n$ | $\ell$ | $L$ | $S$ | $J$ | $\lvert M_J\rvert$ | Label | Energy ($\mathrm{cm}^{-1}$) |
|---|---|---|---|---|---|---|---|
| 1 | 0 | 0 | 1/2 | 1/2 | 1/2 | $^2S_{1/2}$ | 0.0000000000 |
| 2 | 1 | 1 | 1/2 | 1/2 | 1/2 | $^2P_{1/2}$ | 82258.9191133 |
| 2 | 0 | 0 | 1/2 | 1/2 | 1/2 | $^2S_{1/2}$ | 82258.9543992821 |
| 2 | 1 | 1 | 1/2 | 3/2 | 3/2 | $^2P_{3/2}$ | 82259.2850014 |
| 2 | 1 | 1 | 1/2 | 3/2 | 1/2 | $^2P_{1/2}$ | 82259.2850014 |
| 3 | 1 | 1 | 1/2 | 1/2 | 1/2 | $^2P_{1/2}$ | 97492.211200 |
| 3 | 0 | 0 | 1/2 | 1/2 | 1/2 | $^2S_{1/2}$ | 97492.221701 |
| 3 | 2 | 2 | 1/2 | 3/2 | 3/2 | $^2D_{3/2}$ | 97492.319433 |
| 3 | 2 | 2 | 1/2 | 3/2 | 1/2 | $^2D_{3/2}$ | 97492.319433 |
| 3 | 1 | 1 | 1/2 | 3/2 | 3/2 | $^2P_{3/2}$ | 97492.319611 |
| 3 | 1 | 1 | 1/2 | 3/2 | 1/2 | $^2P_{3/2}$ | 97492.319611 |
| 3 | 2 | 2 | 1/2 | 5/2 | 5/2 | $^2D_{5/2}$ | 97492.355566 |
| 3 | 2 | 2 | 1/2 | 5/2 | 3/2 | $^2D_{5/2}$ | 97492.355566 |
| 3 | 2 | 2 | 1/2 | 5/2 | 1/2 | $^2D_{5/2}$ | 97492.355566 |

Table 4.1: Asymptotic atomic basis states of n=1, 2, and 3 of atomic hydrogen from Kramida (2010).[23][24][35][33]

energies are in agreement for $R > 2$ Å, that is outside the maximum in $n = 2$ electron density. At smaller $R$ the failure of the pseudopotential to follow the strongly attractive prediction of the ab initio calculations can be attributed to its incomplete treatment of noble gas structure, and that in this implementation we do not include an attractive interaction at all when the valence electron is inside the noble gas atom's fixed effective cutoff radius. Other pseudopotential calculations (e.g. Baylis (1969) [6]) go to detailed efforts to improve accuracy in this region, but with poor success at improving the result for line shape applications.[29]. Nevertheless, the results are still very useful for longer range, where they match the ab initio calculations well and also provide insight into state mixing. It is of note that the ab initio potentials used by Allard et al in their calculation of the Lyman-$\alpha$ profile and collision-induced effects in its short-wavelength wing do not have the experimental asymptotic energies. This is common to ab initio calculations that use Gaussian basis sets which are insufficient to represent the isolated atom with experimental accuracy. The residual difference is a constant offset that may be ignored when the potentials are used to compute spectra relative to the unperturbed spectral line center, as

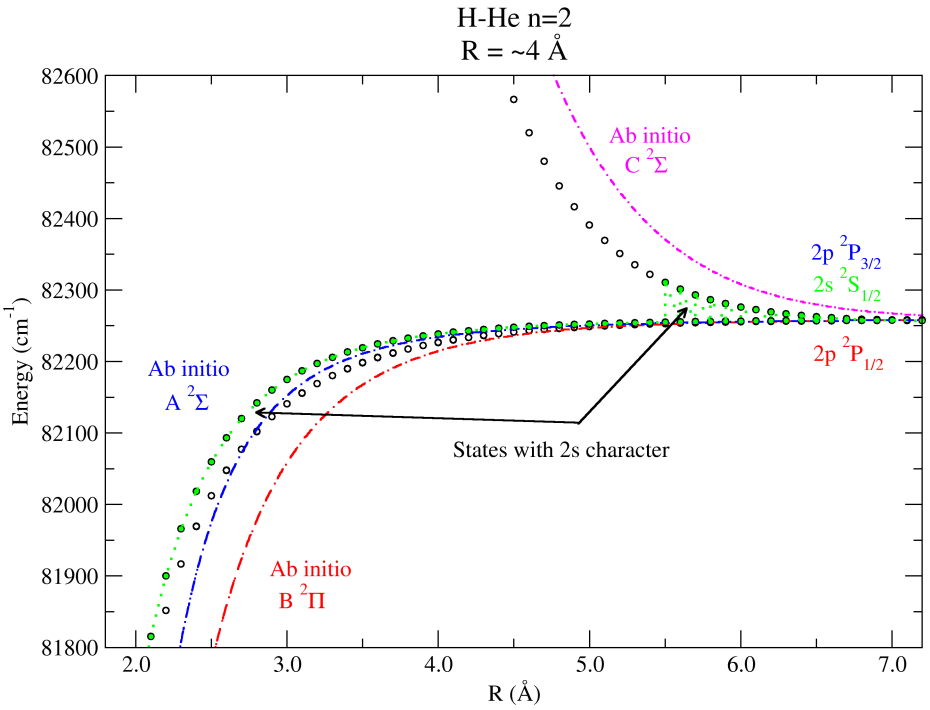


Figure 4.4: The $n = 2$ excited states of an H-He pseudopotential calculation have $R$-dependent mixing with the basis states that are atomic wavefunctions of the isolated atom. State labels from ab initio calculations may not reveal the underpinning character of the state, and the role of the asymptotically forbidden atomic $s \rightarrow s$ transition in determining the dipole transition moment $d(R)$ during a radiative collision. The ab initio calculations in the figure have been shifted downward to match the asymptotic experimental atomic energies.

is the case for Lyman-$\alpha$ in stellar atmosphere models.

In Figs. 4.4, 4.5, 4.6 and Table 4.1 we find that asymptotically there are four atomic states, one from $2s$, and three from $2p$ which is split by spin-orbit coupling. The Lamb shift sets the ordering that puts the $2s$ state above the $2p$ with $J = 1/2$ $M_J = 1/2$ (red dots or lines in the figure). As expected, the $J = 3/2$ $M_J = 3/2, 1/2$ state is highest of the multiplet.

When the van der Waals interaction comes into play, notably closer that 20 Å, there is a separation of the two $M_J$ substates of $J = 3/2$ that *lowers* the $M_J = 3/2$ as we see in Fig. 4.6. In the region around 7 Å the $2s$ state contribution to the state vectors of the eigenstates is shared, and inside that region the $2s$ is only in the downward $A$ and $B$ states that produce the red wing, and not in the upward $C$ state that creates the blue wing.

The van der Waals well in the $2p\ ^2P_{1/2}$ (red) state leads to a mixing region at 7 Å inside of which the ordering is distinct. At 6 Å from high to low we have $2p\,^2P_{3/2}\,1/2$ (magenta), $2p\,^2P_{3/2}\,3/2$ (blue), $2s\,^2S_{1/2}\,1/2$ (green), and $2p\,^2P_{1/2}\,1/2$ (red). That is the same order of states at infinity. However, the potential with the most $2p\,^2P_{3/2}\,3/2$ character, that is the one for which this basis state makes the highest percentage of the wavefunction, connects smoothly to the asymptotic $2p\,^2P_{3/2}\,1/2$ state. While the potential calculations do not adiabatically move the He atom through the H atom's valence charge, the states at each selected $R$ have a specific order and following along R we would "connect the dots" to see which state at large $R$ leads to a state at smaller $R$ without a discontinuity in slope. Consequently, the molecular labels used at small $R$ may be misleading about the parentage at large $R$.

Thus the lowest $n = 2$ states include $2p$ and $2s$, and the $2s$ contribution is largest in the lowest pair which share $M_J = 1/2$ (red and green), while the $M_J = 3/2$ arising from $J = 3/2$ is above them at 6 Å. In the ab initio calculations the lowest state is by convention $A\ ^2\Sigma$. In this region that state correlates to the higher $2p\,^2P_{3/2}\,M_J = 3/2$ state rather than the lower pair (see Fig. 4.5). The $M_J = 3/2$ state continues downward more rapidly with decreasing $R$ than the others, and inside 1.5 Å it is below them. Thus the assignment of $A\,^2\Sigma$ is made on the basis of the order in the so-called "molecular" region of deep wells. It is the state with the most $2s$ character in the $\approx 2$ Å regime as we see Fig. 4.4. In the presence of spin-orbit coupling, this state is a mixture of the $M_J = 1/2$ states arising from the lower $2s\ ^2S_{1/2}\ M_J = 1/2$ and $2p\ ^2P_{1/2}\ M_J = 1/2$ states which closely overlap in the pseudopotential calculations. The result is that transitions from the $B$ state are weakened because the $1s \rightarrow 2s$ transition is not electric-dipole allowed.

The red wing of Lyman-$\alpha$ arises in these calculations from the spatial region between 2 and 5 Å where the He atom encounters the valence electron of the H $n = 2$ state with maximum probability. For the most part, the $2s$ atomic state is the largest component of the states contributing to the

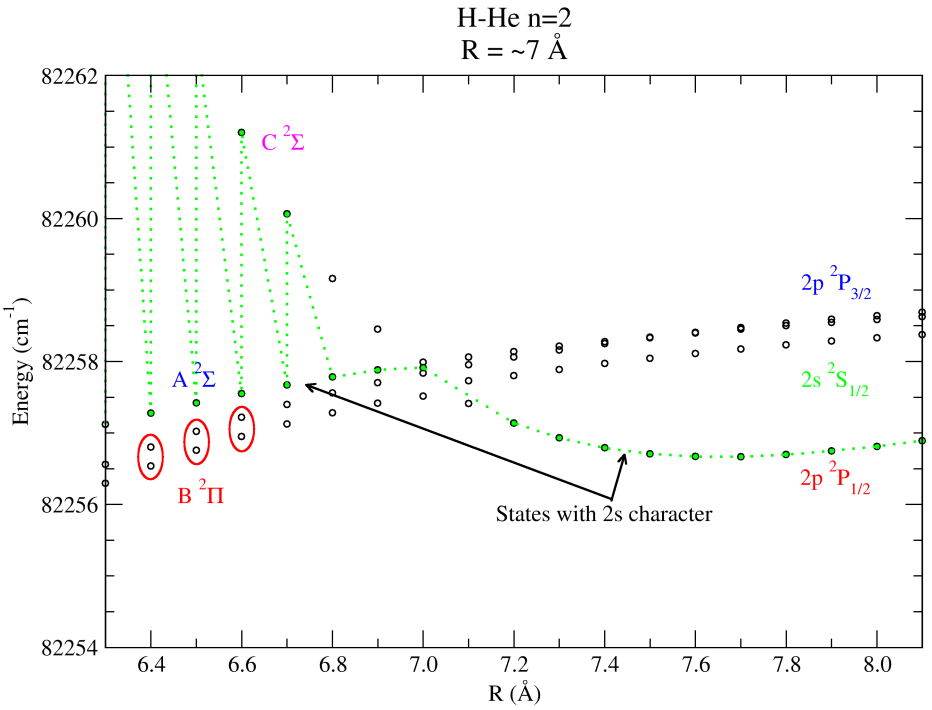


Figure 4.5: In the region of 7 Å separation, the $n = 2$ excited states of an H-He pair approach closely with the 2s state character shared between states with $M_J = 1/2$. Compare to Fig. 4.4 at smaller $R$ and Fig. 4.6 at larger $R$.

red wing in this region. We conclude that the red wing, regardless of the details of the potential and profile, has diminished strength because $d(R)$ is reduced by the $2s$ mixing.

This contrasts with the $C\,^2\Sigma$ state which goes into the 7 Å mixing region from smaller $R$ where it is a mildly repulsive state that produces the blue wing. At $R = 4$ Å this state is 43% $2p\,^2P_{3/2}\,1/2$, with the 35% $2s\,^2S_{1/2}\,1/2$. That is, at small $R$ the state producing the blue wing has $2p$ character and and transitions to it from the ground state are allowed. At about 5 Å the $2s$ component becomes larger than the $2p$, and the transition dipole moment is correspondingly reduced because $1s \rightarrow 2s$ is not allowed. Note the $2s$

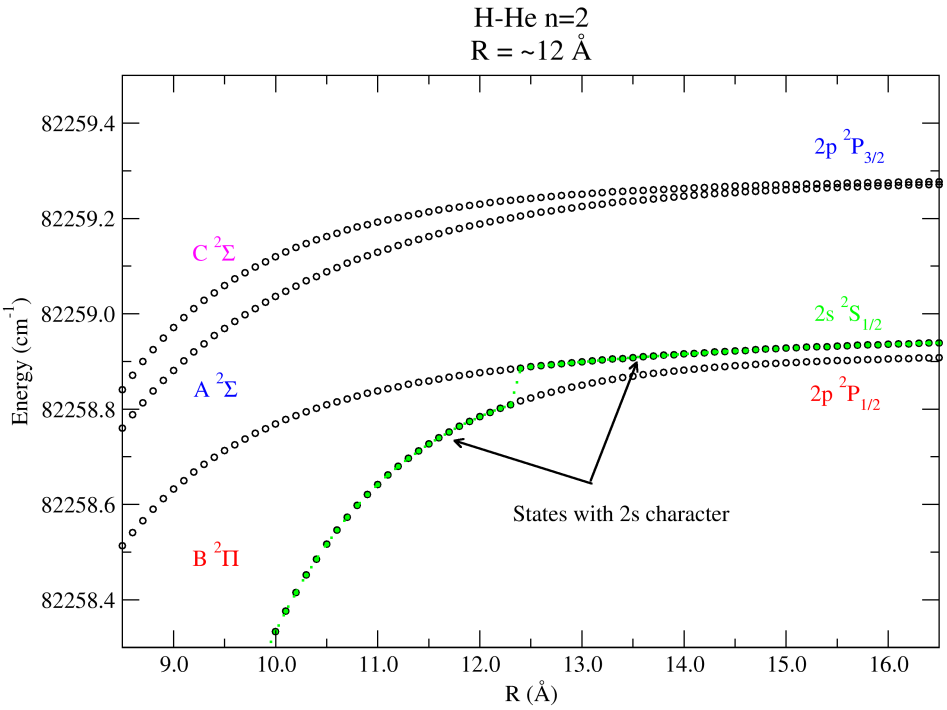


Figure 4.6: Beyond 12 Å the state ordering and the asymptotic atomic parentage are the same. However the $n = 2$ excited states of an H-He pair change their relative character in the vicinity of 12 Å when the asymptotic state with largest $2s$ percentage becomes the lowest state of the multiplet.

character highlighted in Fig. 4.4. In Fig. 4.5 it seems that the $C\,^2\Sigma$ state turns to trend to the $2s\,2S_{1/2}$ atomic state which regains its $2s$ character at 12 Å by interacting with the $2p\,^2P_{1/2}$ state as we see in Fig. 4.6.

The $A$ and $C$ states both have $2s$ character in the 7 Å region as we see in Fig. 4.5 Simply put, in the inner regions the $X- > C$ transition is allowed and has a large $d(R)$ that is determined by the Boltzmann factor from the ground state barrier at smallest $R$. . Spectral features associated with it at short range that arise in the Lyman-$\alpha$ blue wing could be called "collision-induced", in that they arise from changing state mixing and from the Boltzmann factor in close collisions. Asymptotically the atomic tran-

| R (Å) | Energy ($cm^{-1}$) | Label | First | Percent | Second | Percent |
|---|---|---|---|---|---|---|
| 5 | 82248.759 | B | 2 | 0.6837 | 5 | 0.3158 |
| 5 | 82249.006 | B | 4 | 1.0000 | 13 | 0.0000 |
| 5 | 82252.515 | A | 3 | 0.6123 | 5 | 0.2749 |
| 5 | 82390.900 | C | 5 | 0.4089 | 3 | 0.3868 |
| 6 | 82255.391 | B | 2 | 0.7248 | 5 | 0.2703 |
| 6 | 82255.647 | B | 4 | 1.0000 | 13 | 0.0000 |
| 6 | 82256.543 | A | 3 | 0.5816 | 5 | 0.3342 |
| 6 | 82276.307 | C | 3 | 0.4134 | 5 | 0.3955 |
| 7 | 82257.516 | B | 2 | 0.9607 | 5 | 0.0386 |
| 7 | 82257.837 | B | 4 | 1.0000 | 13 | 0.0000 |
| 7 | 82257.913 | C | 3 | 0.8931 | 5 | 0.1053 |
| 7 | 82257.991 | A | 5 | 0.8561 | 3 | 0.1062 |
| 8 | 82256.813 | B | 3 | 0.4593 | 5 | 0.3035 |
| 8 | 82258.331 | C | 2 | 0.7531 | 3 | 0.1996 |
| 8 | 82258.588 | A | 5 | 0.6492 | 3 | 0.3411 |
| 8 | 82258.642 | B | 4 | 1.0000 | 13 | 0.0000 |
| 16 | 82258.905 | B | 2 | 0.9752 | 3 | 0.0245 |
| 16 | 82258.936 | C | 3 | 0.9751 | 2 | 0.0246 |
| 16 | 82259.268 | A | 5 | 0.9994 | 3 | 0.0004 |
| 16 | 82259.275 | B | 4 | 1.0000 | 10 | 0.0000 |

Table 4.2: Examples of percentage basis state mixing at large $R$ in H-He. The basis states are identified by number: (2) $2p\,^2P_{1/2}\,1/2$; (3) $2s\,^2S_{1/2}\,1/2$; (4) $2p\,^2P_{3/2}\,3/2$; (5) $2p\,^2P_{3/2}\,1/2$; (13) $3d\,^2D_{5/2}\,3/2$. The labels are $A\,^2\Sigma$, $B\,^2\Pi$, and $C\,^2\Sigma$ based on similarity to states with labels assigned in the ab initio calculations. [3]

sition of the isolated H atom is forbidden. It is noteworthy that while $2s$ character of the higher potential is decreasing at small $R$, the $2s$ character in the lower pair of downward potentials is increasing. This depresses associated features in the red Lyman-$\alpha$ wing associated with the $A\,^2\Sigma$ and $B\,^2\Pi$ states shown in Fig. 4.4. The disappearance of the red wing and the appearance of the blue wing are related, with the transition probability moving from one side of the line to the other as a consequence of the collision. Table 4.2 breaks down the admixture percentages for the two largest contributions to the eigenstates at long range.

In summary for the $n = 2$ states of H-He the states connect this way/

**X** Is the $1s$ atomic state from infinity into under 1 Å.

**A** Is the lowest of the $n = 2$ states inside 1 Å. In the region where the Lyman-$\alpha$ wings are formed, it is above the $B$ states and below $C$. Asymptotically it goes to $2p\,^2P_{3/2}\,1/2$. At small $R$ it has $2s$ character and transitions to it become forbidden.

**B** Is a double state, split by fine structure, and shows as one state in ab initio calculations without fine structure. The pair of $B$ states are the lowest states in the region where the Lyman-$\alpha$ wing is formed. One of them remains the lowest state at the large $R$ asymptote, corresponding to $2p\,^2P_{1/2}\,1/2$. The other goes to the highest state of the multiplet, corresponding to $2p\,^2P_{3/2}\,1/2$. The $B$ states have transition probability to the ground state at all $R$.

**C** At small $R$ the $C$ state is $2p\,^2P_{3/2}\,1/2$. Transitions to the $C$ state in this close collision region producing the blue wing are allowed. At large $R$ the $C$ state becomes $2s\,^2S_{1/2}\,1/2$ and transitions to it are forbidden.

# Bibliography


[1] N. Allard and J. Kielkopf. The effect of neutral nonresonant collisions on atomic spectral lines. *Reviews of Modern Physics*, 54(4):1103–1182, Oct 1982.

[2] N. F. Allard, A. Royer, J. F. Kielkopf, and N. Feautrier. Effect of the variation of electric-dipole moments on the shape of pressure-broadened atomic spectral lines. *Physical Review A*, 60(2):1021–1033, Aug 1999.

[3] N. F. Allard, S. Xu, J. F. Kielkopf, B. Mehnen, R. Linguerri, G. Guillon, M. Mogren Al Mogren, and M. Hochlaf. H–He collision-induced satellite in the Lyman-$\alpha$ profile of DBA white dwarf stars. *Monthly Notices of the Royal Astronomical Society*, page in press, 2020.

[4] L. U. Ancarani and G. Gasaneo. A simple parameter-free wavefunction for the ground state of three-body systems. *Journal of Physics B Atomic Molecular Physics*, 41(10):105001, May 2008.

[5] L. U. Ancarani, K. V. Rodriguez, and G. Gasaneo. A simple parameter-free wavefunction for the ground state of two-electron atoms. *Journal of Physics B Atomic Molecular Physics*, 40(13):2695–2702, Jul 2007.

[6] W. E. Baylis. Semiempirical, Pseudopotential Calculation of Alkali-Noble-Gas Interatomic Potentials. *Journal of Chemical Physics*, 51(6):2665–2679, Sep 1969.

[7] E. O. Brigham. *The Fast Fourier Transform*. Prentice-Hall, Englewood Cliffs, New Jersey, 1974.

[8] E. Czuchaj and J. Sienkiewicz. Adiabatic Potentials of the Alkali-Rare Gas Atom Pairs. *Zeitschrift Naturforschung Teil A*, 34(6):694–701, Jun 1979.

[9] G. Deridder and W. van Renspergen. Tables of damping constants of spectral lines broadened by H and He. *Astronomy and Astrophysics*, 23:147, Feb 1976.

[10] A. S. Dickinson and F. X. Gadéa. Undulations in potential curves analyzed using the Fermi model: LiH, LiHe, LiNe, and $H_2$ examples. *Physical Review A*, 65(5):052506, May 2002.

[11] E. Fermi. Sopra lo Spostamento per Pressione delle Righe Elevate delle Serie Spettrali. *Il Nuovo Cimento*, 11(3):157–166, Mar 1934.

[12] J. Fraunhofer. Bestimmung des Brechungs- und des Farbenzerstreungs-Vermögens verschiedener Glasarten, in Bezug auf die Vervollkommnung achromatischer Fernröhre. *Denkschriften des Königlichen Akademie der Wissenschaftern zu München*, 5:193–226, 1817. Retrieved 2019-11-23.

[13] B. T. Gänsicke, D. Koester, J. Farihi, and O. Toloza. Broadening of Ly $\alpha$ by neutral helium in DBA white dwarfs. *Monthly Notices of the Royal Astronomical Society*, 481(4):4323–4331, Dec 2018.

[14] P. Gombas. *Pseudopotentiale*. Springer, Berlin, 1967.

[15] I. Hubeny and T. Lanz. A brief introductory guide to tlusty and synspec, 2017.

[16] J. Katriel and E. R. Davidson. Asymptotic Behavior of Atomic and Molecular Wave Functions. *Proceedings of the National Academy of Science*, 77(8):4403–4406, Aug 1980.

[17] J. F. Kielkopf. Semiempirical potentials for alkali-noble gas interactions. *Journal of Chemical Physics*, 61(11):4733–4739, Dec 1974.

[18] J. F. Kielkopf. Measurement of the width, shift and asymmetry of the sodium D lines broadened by noble gases. *Journal of Physics B Atomic Molecular Physics*, 13(19):3813–3821, Oct 1980.

[19] J. F. Kielkopf and N. F. Allard. Observation of the simultaneous additive effect of several xenon perturbers on the Cs 6s-9p doublet. *Physical Review Letters*, 43(3):196–199, Jul 1979.

[20] J. F. Kielkopf and J. A. Gwinn. Semiclassical Theory of Satellite Bands Produced in the Spectra of Alkali Metals by Interaction with Foreign Gases. *Journal of Chemical Physics*, 48(12):5570–5575, Jun 1968.

[21] G. Kirchhoff and M. L. Foucault. On the simultaneous emission and absorption of rays of the same definite refrangibility; being a translation of a paper. *Philosophical Magazine*, 19:193, 1860.

[22] D. Koester. White dwarf spectra and atmosphere models. *Memorie della Societa Astronomica Italiana*, 81:921–931, Jan 2010.

[23] A. Kramida. Erratum to "A critical compilation of experimental data on spectral lines and energy levels of hydrogen, deuterium, and tritium" [At. Data Nucl. Data Tables 96 (2010) 586-644]. *Atomic Data and Nuclear Data Tables*, 126:295–298, Mar 2019.

[24] A. E. Kramida. A critical compilation of experimental data on spectral lines and energy levels of hydrogen, deuterium, and tritium. *Atomic Data and Nuclear Data Tables*, 96(6):586–644, Nov 2010.

[25] H. Kuhn. Pressure Broadening of Spectral Lines and van der Waals Forces. I. Influence of Argon on the Mercury Resonance Line. *Proceedings of the Royal Society of London Series A*, 158(893):212–229, Jan 1937.

[26] H. G. Kuhn. *Atomic Spectra*. Academic Press, New York, 1961.

[27] E. L. Lewis. Collisional relaxation of atomic excited states, line broadening and interatomic interactions. *Physics Reports*, 58(1):1–71, Feb 1980.

[28] E. L. Lewis and L. F. McNamara. Broadening of the D Lines and the Relaxation of the Resonance Levels of Sodium Due to Collisions with Helium. *Physical Review A*, 5(6):2643–2651, Jun 1972.

[29] W. S. Lobb and D. G. McCartan. The accuracy of interatomic potentials in neutral atom line broadening. In L. Frommhold and J. W.

Keto, editors, *American Institute of Physics Conference Series*, volume 216 of *American Institute of Physics Conference Series*, pages 183–184, Dec 1990.

[30] N. Lwin and D. G. McCartan. Collision broadening of the potassium resonance lines by noble gases. *Journal of Physics B Atomic Molecular Physics*, 11(22):3841–3849, Nov 1978.

[31] F. Masnou-Seeuws. Molecular potentials for systems with one or two active electrons. *Journal de Physique*, 46(C1-1):43–58, Jan 1985.

[32] D. G. McCartan and J. M. Farr. Collision broadening of the sodium resonance lines by noble gases. *Journal of Physics B Atomic Molecular Physics*, 9(6):985–994, Apr 1976.

[33] C. E. Moore. *Atomic Energy Levels Volume I, Circular 467*. U.S. Government Printing Office, Washington, D.C., 1949.

[34] J. N. Murrell, T. G. Wright, and D. S. Bosanac. A search for bound levels of the van der waals molecules: $H_2$, HeH, LiH and LiHe. *Journal of Molecular Structure: THEOCHEM*, 591(1):1 – 9, 2002.

[35] National Institute of Standards and Technology (NIST). Atomic energy levels. `https://physics.nist.gov/PhysRefData/ASD/levels_form.html`, 2019. [Online; accessed 2019-11-30].

[36] H. Partridge, D. W. Schwenke, and J. Bauschlicher, Charles W. Theoretical study of the ground states of the rare-gas hydrides, HeH, NeH, and ArH. *Journal of Chemical Physics*, 99(12):9776–9782, Dec 1993.

[37] J. Pascale. Pseudopotential molecular-structure calculations for NaHe and CsHe. *Physical Review A*, 26(6):3709–3712, Dec 1982.

[38] J. Pascale. Use of l-dependent pseudopotentials in the study of alkali-metal-atom-He systems. The adiabatic molecular potentials. *Physical Review A*, 28(2):632–644, Aug 1983.

[39] J. Pascale and J. Vandeplanque. Excited molecular terms of the alkali-rare gas atom pairs. *Journal of Chemical Physics*, 60(6):2278–2289, Mar 1974.

[40] G. Peach. Interatomic potentials and applications to spectral line broadening. *Memorie della Societa Astronomica Italiana Supplementi*, 15:68, Jan 2010.

[41] M. J. Puska, R. M. Nieminen, and M. Manninen. Electronic polarizability of small metal spheres. *Physical Review B*, 31(6):3486–3495, Mar 1985.

[42] J. E. Sansonetti. Wavelengths, Transition Probabilities, and Energy Levels for the Spectra of Sodium (Na I-Na XI). *Journal of Physical and Chemical Reference Data*, 37(4):1659–1763, Dec 2008.

[43] T. Saue, L. Visscher, H.-J. Jensen, and R. Bast. DIRAC, a relativistic ab initio electronic structure program. `http://www.diracprogram.org/`. [Online; accessed 2019-11-27].

[44] L. Szasz. *Pseudopotential Theory of Atoms and Molecules.* Wiley, New York, 1985.

[45] K. T. Tang, J. P. Toennies, and C. L. Yiu. Accurate Analytical He-He van der Waals Potential Based on Perturbation Theory. *Physical 'review Letters*, 74(9):1546–1549, Feb 1995.

[46] A. Unsöld. *Physik der Sternatmosphären, MIT besonderer Berucksichtigung der Sonne.* Springer, 1955.

[47] S. Warnecke, K. T. Tang, and J. P. Toennies. Communication: A simple full range analytical potential for $H_2$ $b\,^3\Sigma_u^+$, $H-He$ $^2\Sigma^+$, and $He_2$ $^1\Sigma_g^+$ . *Journal of Chemical Physics*, 142(13):131102, Apr 2015.

[48] H.-J. Werner. Molpro: Quantum chemistry software. `https://www.molpro.net/`, 2019. [Online; accessed 2019-11-27].

[49] Wikipedia. List of quantum chemistry and solid-state physics software. `https://en.wikipedia.org/wiki/List_of_quantum_chemistry_and_solid-state_physics_software`, 2019. [Online; accessed 2019-11-27].

[50] W. H. Wollaston. A method of examining refractive and dispersive powers by prismatic reflection. *Philosophical Transactions of the Royal Society*, 92:365–380, 1802. Retrieved 2019-11-23; cited by Wikipedia: ; see page 378 for the specific description of the spectrum.